

Conductance Fluctuations and Chaotic Scattering in Ballistic Microstructures

C. M. Marcus,⁽¹⁾ A. J. Rimberg,⁽¹⁾ R. M. Westervelt,⁽¹⁾ P. F. Hopkins,⁽²⁾ and A. C. Gossard⁽²⁾

⁽¹⁾Division of Applied Sciences and Department of Physics, Harvard University, Cambridge, Massachusetts 02138

⁽²⁾Materials Department, University of California, Santa Barbara, California 93106

(Received 9 January 1992)

We report detailed measurements of the low-temperature magnetoconductance in ballistic microstructures in the shape of a "chaotic" stadium and a circle with quantum-point-contact leads. Both structures show large, aperiodic, conductance fluctuations as a function of perpendicular magnetic field, and a zero-field resistance peak indicating geometry-dependent enhanced backscattering. Power spectra of fluctuations are consistent with recent semiclassical analyses based on quantum chaotic scattering, with the circle showing enhanced high-frequency spectral content.

PACS numbers: 73.20.Dx, 05.45.+b, 72.20.My, 73.20.Fz

The advent of precision submicron lithography provides a means of investigating electron transport in the ballistic regime, where the mean free path of the electrons exceeds the size of the device [1,2]. Recent experiments [3] on semiconductor microstructures have uncovered a variety of interesting transport "anomalies" all of which demonstrate the importance of geometrical features in determining transport in the ballistic regime. These anomalies have been analyzed quite successfully in terms of classical "billiard ball" models which consider transport to be governed by the deterministic scattering of classical electrons from the confining walls of the microstructure [2,4]. At very low temperatures ($T \lesssim 0.5$ K) quantum interference effects become important, giving rise to large fluctuations in transport [5], reminiscent of universal conductance fluctuations (UCF) [6]. Quantum interference effects in the ballistic regime are not described by classical billiard ball models [2,4], nor are they addressed by the current theories of UCF [6] and weak localization [7], which are specifically suited to disordered metallic systems in which electrons move diffusively.

Recent theoretical work [8-11] has addressed the statistical properties of fluctuations in ballistic transport within the semiclassical framework of quantum chaotic scattering [12]. In this formulation, electrons follow classical trajectories and move ballistically between wall collisions, but also carry phase information that depends on the Fermi energy and is affected, for instance, by a magnetic vector potential as in the Aharonov-Bohm (AB) effect. Transport is then treated as a scattering problem characterized by a matrix t_{nm} of complex transmission amplitudes connecting incoming and outgoing channels. When the associated classical scattering is chaotic, t_{nm} is found to possess certain universal statistical properties [8-10] that can be related to the statistics of conductance fluctuations through the Landauer formula, $G = (2e^2/h) \sum_{m,n=1}^N |t_{mn}|^2$, where N is the number of quantum channels in the incoming and outgoing leads [13]. A semiclassical analysis along these lines has also recently been applied to fluctuations observed in the reflectivity of "chaotic" microwave cavities [14].

In this Letter, we experimentally investigate the low-temperature magnetotransport of ballistic semiconductor

"quantum dots." These submicron structures, shown as insets in Fig. 1, exhibit aperiodic conductance fluctuations as a function of an applied perpendicular magnetic field for modest fields, $B < 0.3$ T. We find that power spectra of these fluctuations agree well with predictions of semiclassical chaotic scattering theory [8,9], and also reveal significant dependences on geometry. We also observe a resistance peak at zero field that suggests a ballistic enhanced backscattering effect analogous to weak localization in disordered systems. In addition, we see shape-dependent periodic components in the transmission which are signatures of unstable periodic orbits in the structures. Finally, we observe that the amplitude of the fluctuations are not "universal" in that they are smaller and increase with the average conductance as the point contacts are opened.

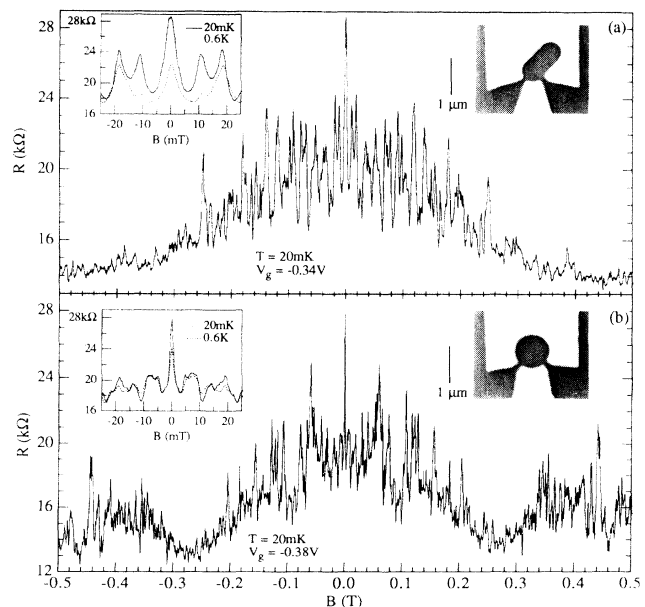


FIG. 1. Resistance R as a function of perpendicular magnetic field B for (a) stadium 1, (b) circle 1, both with $N=1$ fully transmitted modes in leads. Insets: Zero-field peaks at 20 mK (solid) and 0.6 K (dashed), and electron micrographs of devices, with $1 \mu\text{m}$ bar for scale.

The specific shapes of the microstructures, denoted “stadium” [Fig. 1(a)]—semicircles connected by straight edges—and “circle” [Fig. 1(b)] were chosen to emphasize the connection between ballistic transport and billiard models of quantum chaos [14] and to allow a comparison of fluctuation phenomena in ballistic structures whose classical scattering in the corresponding *idealized* structures is chaotic (the stadium) versus non-chaotic (the circle). It is interesting to note that standard UCF can also be considered an example of quantum chaos associated with complex electron trajectories caused by randomly located scatterers [6]. This experiment illustrates that similar fluctuation phenomena can be produced by quantum chaos associated with the *shape* of the conductor; these fluctuations would be present in ideal conductors even in the absence of impurity scattering.

The quantum dots were fabricated using electrostatic gates on the surface of a GaAs/Al_{0.3}Ga_{0.7}As heterostructure. The material was grown with the two-dimensional electron gas (2DEG) very close to the surface (420 Å total distance, with Si δ doping, $N_D = 6 \times 10^{12} \text{ cm}^{-2}$, set back 200 Å from the 2DEG), giving a steep-walled potential from the gates at the level of the 2DEG and preserving the precise dot geometry. Gates are Au/Cr (80 Å/20 Å) patterned using electron-beam lithography and liftoff. Van der Pauw transport measurements at 20 mK with gates grounded gave a sheet density $n_s = 3.8 \times 10^{11} \text{ cm}^{-2}$ and mobility of 265 000 cm²/Vs, from which we infer an elastic mean free path of 2.6 μm —several times the size of the structures. At low temperatures, small-angle scattering due to charged impurities located outside the well is important [15]. While the associated potential fluctuations in the plane of the electron gas are largely screened, electron trajectories are bent by the induced density fluctuations as well as by the residual unscreened potential [16]. As shown below, the influence of dot shape is robust to these small-angle deviations.

The stadium and circle are fabricated close together (10 μm separation) on a single sample and simultaneous four-probe measurements of the two devices are made via six In Ohmic contacts at the edges of the sample. Data from two nominally identical samples, denoted 1 and 2, are reported here. The lithographic dimensions of the quantum dots are as follows. Circle, radius 0.44 μm ; stadium, length 1.2 μm and width 0.60 μm ; all lead widths are 0.14 μm . Effective areas of the confined 2DEG’s are smaller than these lithographic dimensions because of edge depletion, and can be measured directly from periodic AB conductance oscillations [17] at larger fields, $B > 1 \text{ T}$, where well-formed edge states exist. The areas inferred from AB oscillations are 0.41 μm^2 for both the circle and the stadium. This size sets two characteristic magnetic fields, a characteristic field for quantum interference $B_{\text{qm}} \sim \Phi_0/\text{area} = 10 \text{ mT}$ (where Φ_0 is the quantum of flux $h/e = 4.14 \times 10^{-3} \text{ T}\mu\text{m}^2$), and a classical characteristic field $B_{\text{cl}} \sim 0.3 \text{ T}$, for which the classical cy-

clotron radius $l_{\text{cycl}} = \hbar(2\pi n_s)^{1/2}/eB$ is comparable to the size of the structure.

The leads in each device form quantum point contacts oriented at 90° to reduce transmission via direct trajectories. The number N of transverse modes in the leads can be inferred from the zero-field conductance $G(0)$ as a function of gate voltage V_g , which shows oscillations over the range $V_g \sim -0.3 \text{ V}$ to $\sim -0.6 \text{ V}$. Because the leads are rather narrow, $N \leq 3$ for all leads, consistent with estimates based on the depleted lead width and Fermi wavelength $\lambda_F = (2\pi/n_s)^{1/2} = 41 \text{ nm}$ [2].

Transport measurements were carried out in a dilution refrigerator using standard ac lock-in techniques. Current sources of either 0.1 to 0.25 nA at 11 Hz were used, depending on the resistance of the device, and showed no significant difference. Each device has two point contacts and is measured in a four-probe configuration to avoid contribution from the electrical leads. Because nearly all of the measured voltage is dropped across the quantum dot, one can consider this configuration to be a two-probe measurement of the dot. This is significant in considering the $\pm B$ symmetry of the magnetoconductance described below.

Resistances $R(B)$ [$=G^{-1}(B)$] of stadium 1 and circle 1 as a function of perpendicular magnetic field are shown in Fig. 1. For the gate voltages used in this sweep (see Fig. 1) the number of fully transmitted modes in each of the leads is $N=1$, with some tunneling of the second mode contributing to the conductance. Both the stadium and the circle show large aperiodic resistance fluctuations at low fields, $|B| \lesssim 0.3 \text{ T}$, which are reproducible to within 2% as long as the sample is kept at low temperature. Depending on the particular gate voltage, these fluctuations may persist to higher fields ($|B| > 1 \text{ T}$), gradually becoming dominated by a single period due to AB interference of edge states [17]. The traces in Fig. 1 are essentially symmetric, $R(B) \approx R(-B)$, which is expected for a two-probe measurement [13]; small deviations from symmetry are presumably due to voltage drops in the bulk 2DEG, away from the microstructures.

Both traces in Fig. 1 show narrow resistance peaks at $B=0$ which persist to above 0.6 K (see insets). At other gate voltages as well, $R(B)$ is always found to be a local maximum at $B=0$ whenever $N \geq 1$, though zero-field peaks are not always as strong as those in Fig. 1. Specifically, the zero-field peak becomes less pronounced as the leads are opened. The physical origin of the zero-field peak is presumably coherent backscattering associated with interference of time-reversed paths, as for weak localization in diffusive electron systems. We emphasize, however, that no detailed theory of enhanced backscatter for a ballistic quantum dot geometry has appeared. The FWHM’s of the zero-field resistance peaks (see Fig. 1 insets) are 4 mT for stadium 1 and 1.5 mT for circle 1, comparable to the estimate $B_{\text{qm}}/2\pi \approx 1.6 \text{ mT}$ based on time-reversed path arguments, assuming loop areas on the order of device size. Notice that the zero-field peak is

considerably narrower for the circle indicating that the flux enclosed by a typical closed-loop trajectory is larger for the circle than for the stadium. A similar geometrical effect also appears as enhanced high-frequency content in the power spectrum of the circle (discussed below) and is associated with large-area *circulating* orbits [11].

Broad resistance minima around $B \sim \pm 0.27$ T for the circle [Fig. 1(b)] can be interpreted as due to the curvature of electron trajectories. When l_{cycl} equals the dot radius r the point contacts are connected by a directly “aimed” (though not focused) trajectory. This feature allows us to measure the effective sheet density n_{dot} *within the dot*. Using $r = 0.36 \mu\text{m}$ (from AB oscillations) gives $n_{\text{dot}} = 3.5 \times 10^{11} \text{cm}^{-2}$, a slight reduction from the bulk $n_s = 3.8 \times 10^{11} \text{cm}^{-2}$. The absence of a similar feature for the stadium is not a general observation; characteristic dips in $R(B)$ are seen for the stadium at other gate voltages. We expect, however, that this feature will be stronger in the circle, since the condition $l_{\text{cycl}} = r$ causes electrons originating in *either* lead to arrive at the other point contact, either directly or via two wall bounces. No such “double aiming” condition exists for our stadium.

Next we consider the statistics of the conductance fluctuations by evaluating the power spectrum S_g of $\delta g(B)$, the fluctuating part of the dimensionless conductance $g(B) = (h/e^2)G(B) \approx (25.8 \text{ k}\Omega)G(B)$. Conductance fluctuations $\delta g(B)$ are extracted from $g(B)$ by subtracting a third-order polynomial fit to $g(B)$. This suppresses large slowly varying field dependences in conductance, and affects only the lowest-frequency components of S_g . Heuristically, the abscissa of the power spectrum, the magnetic “frequency” f (in units of cycles/T), can be expressed as an area by the AB relation, $\text{area} = \Phi_0 f$, so the spectrum measures the distribution of flux areas of trajec-

tories contributing to conduction [18]. Averaged power spectra [19] for the two samples are shown in Fig. 2 for the case of $N=3$ transverse modes in the leads. Also shown is the autocorrelation function $C(\Delta B) = \langle \delta g(B)\delta g(B+\Delta B) \rangle$, which is the Fourier transform of S_g .

Semiclassical theory [8,9] predicts the universal form $C(\Delta B) = C(0)/[1 + (\Delta B/\alpha\Phi_0)^2]^2$ assuming an exponential distribution of classical trajectory areas A within the structure, $N(A) \propto \exp(-2\pi\alpha|A|)$ [8]. This form for $C(\Delta B)$ should apply when the classical scattering is chaotic (which requires $|B| < B_{\text{cl}}$ for the stadium, and in principle does not apply to the circle) and when the number of modes in the leads is large, $N \gg 1$. It is expected [9,12], however, that this form will be reasonably accurate in the few-mode case. The associated prediction for the power spectrum is

$$S_g(f) = S_g(0)[1 + (2\pi\alpha\Phi_0)f]^2 e^{-(2\pi\alpha\Phi_0)f}, \quad (1)$$

where, again, f is the magnetic frequency in cycles/T. A two-parameter least-squares fit by Eq. (1) using the stadium spectrum gives the solid curves in Fig. 2. These fits yield a characteristic field $\alpha\Phi_0 = 3.6$ mT (3.9 mT), comparable to the width of the zero-field peak, and $\alpha^{-1} = 1.2 \mu\text{m}^2$ ($1.1 \mu\text{m}^2$) for stadium 1 (2). Expressing α^{-1} in terms of the area of the stadium gives $\alpha^{-1}/\text{area} \approx 2.8$ (2.6), consistent with numerical results of Jalabert, Baranger, and Stone [8]. Note that the form of Eq. (1) is in good agreement with the measured stadium spectra over roughly 3 orders of magnitude in power.

At low frequencies, $f < 250$ cycles/T, the circle spectrum coincides with the stadium spectrum and is also consistent with Eq. (1). Above this frequency, the circle spectrum lies significantly above the theoretical curve and the stadium spectrum. This difference was also observed

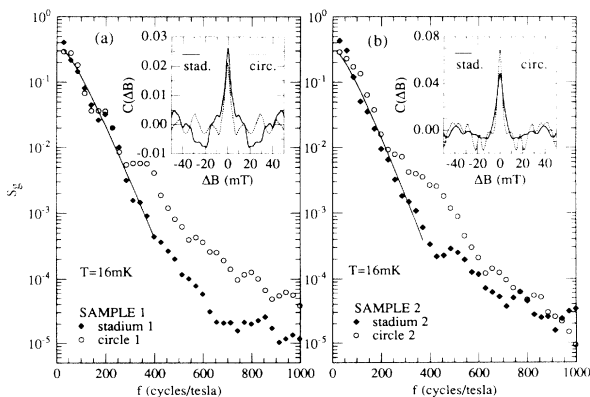


FIG. 2. Averaged power spectra S_g of conductance fluctuations $\delta g(B)$ for stadium (solid diamonds) and circle (open circles) with $N \sim 3$ transverse modes in leads [20]. (a) Sample 1; (b) sample 2. Solid curves are fits of semiclassical theory, Eq. (1), to stadium data. Insets: Autocorrelation $C(\Delta B)$ of stadium (solid) and circle (dashed) for $0.01 \text{ T} < B < 0.29 \text{ T}$, with normalization $C(0) = \text{var}[g(B)]$.

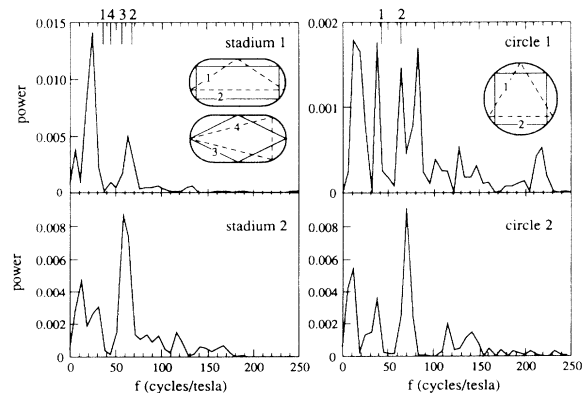


FIG. 3. Low-frequency structure appears in unaveraged spectra of low-field $\delta g(B)$ when plotted on a linear scale [20]. All data for $N \sim 3$ transverse modes in leads. Insets: Symmetric periodic orbits of ≤ 4 bounces with nonzero flux for circle and stadium, with associated frequencies indicated on graphs. Note that many other closed orbits exist in both structures [22].

in a recent theoretical study comparing chaotic and non-chaotic junctions [11] and can be attributed to the nonexponential distribution of areas in the circle. In particular, the circular billiard conserves angular momentum, thus trajectories will sweep out areas at a constant rate rather than randomly as for chaotic billiards [10,11]. This leads to an enhanced number of large-area (i.e., high-frequency) trajectories in the circle. In real devices, disorder will bend trajectories so that angular momentum will not be strictly conserved. However, for predominantly small-angle scattering, the argument for an enhanced number of large-area trajectories in the circle remains applicable.

The averaged spectra in Fig. 2 only address statistical aspects of conductance fluctuations. Geometry-specific structure appears at low frequencies when the spectra are not averaged [19], and are plotted with linear ordinate, as shown in Fig. 3. These features are also visible as periodic oscillations in $R(B)$ (Fig. 1) and in $C(\Delta B)$ (Fig. 2, inset). The large spectral features are a clear signature of the ballistic regime [5], where transport can be dominated by a few preferred trajectories with well-defined areas. This phenomenon is analogous to "scarring" of the wave function by periodic orbits in closed billiards [20]. Figure 3 shows that the largest spectral peaks are concentrated below $f=100$ cycles/T, corresponding to the dot area, and that spectral peaks appear at similar frequencies in the two samples though with different amplitudes. In principle, large spectral peaks of this sort can be associated with simple periodic orbits (insets of Fig. 3). With the present data, however, we do not believe that it is possible to specifically assign the peaks in Fig. 3 to particular orbits. Such an assignment is complicated by disorder, field-dependent curvature of electron trajectories which limits the usable field range, and how well the periodic orbits couple into the leads of the device.

Finally, we observe that the fluctuation amplitude is not independent of the average conductance $\langle g \rangle$ through the device, but increases with conductance as the leads are opened by changing gate voltage. For the circle and stadium in both samples, $\text{rms}(\delta g) \sim 0.1 \langle g \rangle$ for $0.5 < \langle g \rangle < 3$, and $\text{rms}(\delta g)$ vs $\langle g \rangle$ appears slightly concave down. This dependence is characteristic of laser speckle [21], and contrasts UCF, where $\text{rms}(\delta g) \sim 1$ independent of $\langle g \rangle$.

The authors thank B. Altshuler, H. Baranger, R. Jalabert, and R. Jensen for informative discussions. C.M.M. acknowledges financial support as an IBM postdoctoral fellow. Research supported at Harvard by the ONR under N00014-89-J-1592 and N00014-89-J-1023 and the NSF under DMR-91-19386, and at UCSB by the AFOSR under 91-0214.

[1] *Nanostructure Physics and Fabrication*, edited by M. A. Reed and W. P. Kirk (Academic, New York, 1989).

- [2] C. W. J. Beenakker and H. van Houten, in *Solid State Physics*, edited by H. Ehrenreich and D. Turnbull (Academic, San Diego, 1991), Vol. 44.
- [3] M. L. Roukes *et al.*, Phys. Rev. Lett. **59**, 3011 (1987); G. Timp *et al.*, Phys. Rev. Lett. **60**, 2081 (1988); C. J. B. Ford, Phys. Rev. Lett. **62**, 2724 (1989); A. M. Chang, T. Y. Chang, and H. U. Baranger, Phys. Rev. Lett. **63**, 996 (1989).
- [4] C. W. J. Beenakker and H. van Houten, Phys. Rev. Lett. **63**, 1857 (1989); in *Electronic Properties of Multilayers and Low-Dimensional Semiconductor Structures*, edited by J. M. Chamberlain, L. Eaves, and J. C. Portal (Plenum, London, 1990).
- [5] G. Timp *et al.*, Phys. Rev. Lett. **59**, 732 (1987); A.M. Chang *et al.*, Phys. Rev. **B 37**, 2745 (1988); C. J. B. Ford *et al.*, Surf. Sci. **229**, 298 (1990).
- [6] B. L. Altshuler, Pis'ma Zh. Eksp. Teor. Fiz. **41**, 530 (1985) [JETP Lett. **41**, 648 (1985)]; P. A. Lee and A. D. Stone, Phys. Rev. Lett. **55**, 1622 (1985); B. L. Altshuler and B. I. Shklovskii, Zh. Eksp. Teor. Fiz. **91**, 220 (1986) [Sov. Phys. JETP **64**, 127 (1986)].
- [7] G. Bergmann, Phys. Rep. **107**, 1 (1984).
- [8] R. A. Jalabert, H. U. Baranger, and A. D. Stone, Phys. Rev. Lett. **65**, 2442 (1990).
- [9] E. Doron, U. Smilansky, and A. Frenkel, Physica (Amsterdam) **50D**, 367 (1991).
- [10] R. V. Jensen, Chaos **1**, 101 (1991).
- [11] R. B. S. Oakeshott and A. MacKinnon, Superlattices Microstr. **11**, 145 (1992).
- [12] U. Smilansky, in *Chaos and Quantum Physics*, edited by M.-J. Giannoni, A. Voros, and J. Zinn-Justin (Elsevier Science, London, 1990); C. H. Lewenkopf and H. A. Weidenmüller, Ann. Phys. (N.Y.) **212**, 53 (1991); E. Doron and U. Smilansky, Phys. Rev. Lett. **68**, 1255 (1992).
- [13] R. Landauer, IBM J. Res. Dev. **1**, 223 (1957); M. Büttiker, IBM J. Res. Dev. **32**, 317 (1988).
- [14] H.-J. Stöckmann and J. Stein, Phys. Rev. Lett. **64**, 2215 (1990); E. Doron, U. Smilansky, and A. Frenkel, Phys. Rev. Lett. **65**, 3072 (1990).
- [15] Shubnikov-de Haas oscillations measured at 0.3 K in a Hall bar fabricated from the same wafer give single particle lifetimes $\tau_s \sim 0.07 \tau_\mu$, where τ_μ is transport scattering time, consistent with theory [S. Das Sarma and F. Stern, Phys. Rev. **B 32**, 8442 (1985)] and previous experiments on GaAs heterostructures [J.P. Harring *et al.*, Phys. Rev. **B 32**, 8126 (1985); F. Fang *et al.*, Surf. Sci. **196**, 310 (1988)]. This suggests that mobility in our material is limited primarily by small-angle scattering.
- [16] J. A. Nixon and J. H. Davies, Phys. Rev. **B 41**, 7929 (1990).
- [17] B. J. van Wees *et al.*, Phys. Rev. Lett. **62**, 2523 (1989).
- [18] R. P. Taylor *et al.*, Surf. Sci. **196**, 52 (1988).
- [19] Spectra in Fig. 2 are averages of 15 FFT (fast Fourier transform) power spectra from half-overlapping 256-point blocks in the range $0.01 \text{ T} < B < 0.29 \text{ T}$, normalized to $\sum_i^{256} S_g(f_i) = 1$. Data in Fig. 3 are single FFT spectra using 1024-point blocks in the range $|B| < 0.07 \text{ T}$.
- [20] E. J. Heller, Phys. Rev. Lett. **53**, 1515 (1984).
- [21] S. Feng *et al.*, Phys. Rev. Lett. **61**, 834 (1988).
- [22] M. C. Gutzwiller, *Chaos in Classical and Quantum Mechanics* (Springer, New York, 1990).

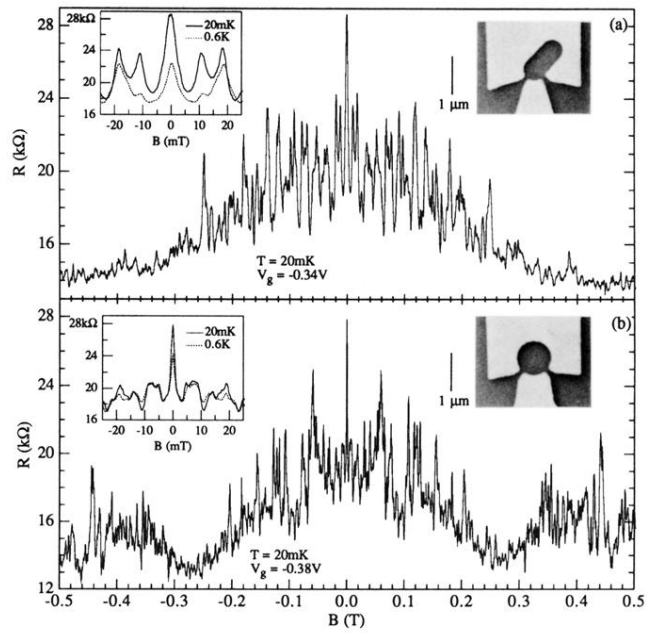


FIG. 1. Resistance R as a function of perpendicular magnetic field B for (a) stadium 1, (b) circle 1, both with $N=1$ fully transmitted modes in leads. Insets: Zero-field peaks at 20 mK (solid) and 0.6 K (dashed), and electron micrographs of devices, with $1\ \mu\text{m}$ bar for scale.